

Towards Mo/Au based TES detectors for Athena/X-IFU

Lourdes Fàbrega*^a, Agustín Camón^b, José Luís Costa-Krämer^c, Carlos Pobes^b, María Parra-Borderías^{d,e}, Iván Fernández-Martínez^f, Rosa Jáudenes^c, Pedro Cereceda^c, María Teresa Ceballos^g, Xavier Barcons^g, Javier Sesé^h, Jesús Martín-Pintado^e, Luciano Gottardiⁱ, Marcel Bruijnⁱ, Madhu Jambunathanⁱ, Roland H. den Hartogⁱ, Jan van der Kuurⁱ, Jan-Willem den Herderⁱ, Didier Barret^{j,k}

^aICMAB-CSIC, Campus de la UAB, Bellaterra, 08193 Spain;

^bICMA, CSIC-Universidad de Zaragoza, Pedro Cerbuna 12, 50009 Zaragoza, Spain;

^cIMM-CSIC, Isaac Newton 8, 28760 Tres Cantos, Spain;

^dIRIS, Parc Mediterrani de la Tecnologia, Avda C.F. Gauss 11, 08860 Castelldefels, Spain;

^eCentro de Astrobiología, CSIC-INTA, 28850 Torrejón de Ardoz, Spain;

^fNano4energy SLNE, c/o ETSII-UPM, José Gutiérrez Abascal 2, 28006Madrid, Spain;

^gIFCA, CSIC-Universidad de Cantabria, Avda. Los Castros s/n, 39005 Santander, Spain;

^hINA and LMA, Universidad de Zaragoza, Mariano Esquillor s/n, 50018 Zaragoza, Spain;

ⁱSRON, Sorbonnelaan 2, 3584 CA Utrecht, Netherlands;

^jUniversité de Toulouse, UPS-OMP, IRAP, Toulouse, France;

^kCNRS, IRAP, 9 Av. Colonel Roche, BP 44346, 31028 Toulouse cedex 4, France;

ABSTRACT

The X-ray spectroscopy telescope *Athena* has been designed to implement the science theme "the hot and energetic universe", selected by the European Space Agency as the second large mission of its Cosmic Vision program. X-IFU, one of the two interchangeable focal plane instruments of *Athena*, is a high resolution X-ray spectrometer made of a large array of Transition Edge Sensors. Two options are under consideration for the X-IFU microcalorimeters: Ti/Au bilayers or Mo/Au bilayers. Here we report on our efforts to develop Mo/Au-based TES. The TES are made of high quality superconducting Mo/Au bilayers fabricated at room temperature on low stress Si₃N₄ membranes; Mo is deposited by RF magnetron sputtering and in-situ covered by a thin (15nm) Au layer deposited by DC sputtering; in a second step, the Au layer thickness is increased ex-situ by e-beam deposition, to obtain suitable resistance R_n and operation temperature values. Very sharp transitions (~few mK transition width) are obtained, with typically R_n~25mΩ and T_c~100-120mK for 65/215 bilayers. First simple TES designs are being tested. Also, Bi films several μm thick, intended to constitute the X-ray absorber, are fabricated by electrochemical deposition.

Keywords: microcalorimeter, *Athena*, Transition Edge Sensor, X-ray

1. INTRODUCTION

The *Athena* mission (Advanced Telescope for High Energy Astrophysics) has been designed to implement the science theme "The Hot and Energetic Universe"¹ that the European Space Agency (ESA) selected for the second large-class mission within the ESA's Cosmic Vision science program. *Athena* will consist of a single X-ray telescope with two interchangeable focal plane instruments, one of them being X-IFU (X-ray Integral Field Unit), a revolutionary X-ray high-spectral resolution cryogenic imager². The X-IFU is the instrument that *Athena* will use to meet some key science goals, in particular detecting weak absorption lines produced by filaments in the Warm-Hot Intergalactic Medium³, to measure bulk velocities and turbulence in the hot diffuse gas trapped in the potential wells of evolving groups and clusters of galaxies⁴, or to diagnose gas physical conditions in a variety of astrophysical environments^{5,6} using He-like emission line triplets. A key scientific requirement for the X-IFU to achieve the above (and other) scientific objectives is the spectral resolution, which is required to be 2.5 eV at X-ray energies below 6 keV.

The X-IFU is a state-of-the-art challenging instrument, as emphasized by Ravera et al.² One of the key ingredients is the front-end sensor array, part of the detector system integrated in the focal plane assembly. This sensor will be constituted by 3840 Transition Edge Sensors (TES), made of superconducting sensors with an X-ray absorber on top of them. The superconducting element, acting as a microcalorimeter, is a proximity bilayer with operation temperature $\sim 100\text{mK}$. Two options are under consideration for the X-IFU microcalorimeters: Ti/Au bilayers⁷ or Mo/Au bilayers. These two materials have been shown to provide the X-ray spectrometers with the highest spectral resolution so far^{7,8,9}, and are therefore the best possible candidates to meet the overall spectral resolution requirements of X-IFU.

In previous work we demonstrated our ability to fabricate high quality, reproducible Mo thin films and Mo-based TES^{10,11,12,13}. Now we have devised a development plan aimed at fabricating TES meeting X-IFU requirements. Here we provide an overview of the progress achieved so far and describe the development plan for the immediate future.

2. FABRICATION

2.1 TES fabrication

Silicon nitride membranes are fabricated using silicon wafers from Si-Mat (diameter 100 mm, orientation $\langle 100 \rangle$, thickness 500 μm , P/Boron doped with resistivity 1-30 Ωcm , polished on both sides and with a coating of 1000 nm low stress silicon nitride). A photolithography process is used to open windows on the silicon nitride with a RIE machine with SF_6 . Then the wafer is mounted on a PEEK wafer holder from AMMT that protects one of the sides and is introduced in a KOH bath (concentrated at 30% and at a temperature of 70 $^\circ\text{C}$); an internal illumination of the AMMT holder is used. The KOH process is stopped when a bright white light is seen through the membranes, which occurs approximately after 7 hours. Finally the wafer is rinsed in purified water several times to avoid residues from KOH in the surface.

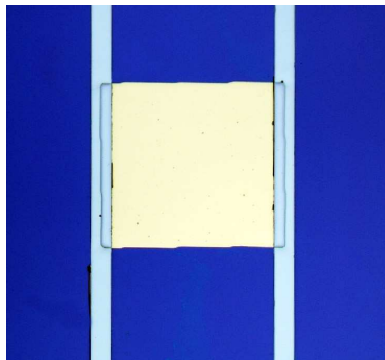


Figure 1. Optical micrograph of one of our Mo/Au TES. Wiring is made of Mo; the four edges of the square are covered by Au, as described in the text.

Mo/Au bilayers are deposited on Si_3N_4 membranes in a UHV chamber at room temperature. RF magnetron sputtering in 5 μbar Ar pressure is used for Mo deposition. Si_3N_4 is cleaned with a KOH solution prior to deposition. This cleaning procedure and base pressure are crucial for the reproducibility and high quality of Mo, while bias voltage during sputtering controls the film stress, ultimately determining its T_c and residual resistance ratio¹¹. After Mo deposition, the pressure is changed to 6 μbar and a 15nm-thick Au film is deposited in-situ by DC magnetron sputtering; typical deposition rates are respectively 0.2nm/s and 0.5nm/s for Mo and Au. The Au layer deposition up to the designed thickness is completed ex-situ by e-beam. This procedure, which we call “trilayer solution”^{10,12}, ensures that the normal resistance of the bilayer is low enough, while preserving the proximity effect, which requires in-situ covering of Mo layer; high resolution Transmission Electron Microscopy displayed no apparent interface between both Au layers¹⁰. Mo and Au depositions by sputtering are done in a dedicated UHV chamber, used exclusively for this project in order to guarantee the absence of any contamination which would severely affect the performances of the TES. Typical thicknesses to obtain $T_c \sim 100\text{mK}$ are 60nm/215nm. These bilayers have been shown¹³ to be stable when heated up to a temperature of 150 $^\circ\text{C}$, which guarantees that they will meet any thermal qualification tests.

The Mo/Au bilayers are patterned after deposition, using selective standard optical lithography by wet chemical etching, to get detectors with lateral size 200 μ m. First, the Au layer is etched using a KI/I solution. Afterwards, the Mo layer is etched in a H₃PO₄/HNO₃/H₂O₂/DI solution, which is selective to Au. Lateral Mo etching is 20 times faster than vertical etching, producing an Au overhang that covers Mo edges^{10,12}, producing in a rather simple way the banks that have been demonstrated essential to obtain sharp and reproducible transitions¹⁴. After this, Mo pads 200nm thick (critical current above 3mA) are deposited by RF sputtering.

2.2 Electrochemical deposition of Bi films

Bi films several microns thick are deposited by electroplating, to be used as absorbers. Several plating solutions have been tested, both aqueous and EDTA-based; some of them are still being subject to optimization. Here we report on what has been obtained using a Bi³⁺ 7.5 10⁻³ M solution in 1.0 M HNO₃, with a reference electrode Ag/AgCl (3M NaCl) and at room temperature.

For the absorber optimization procedure, the substrate is glass, covered by a thin (20nm) Au layer deposited by e-beam; a 2nm Cr adherence layer is previously deposited. This very small thickness of the Au/Cr metallic layer allows measuring the Bi resistance, which we use as a proxy to optimize thermal conductance, since electrical and thermal conductances are proportional at constant temperature, according to the Wiedemann-Franz law.

3. CHARACTERIZATION

3.1 Transition-Edge Sensors

Measurements are performed in a commercial dilution refrigerator (Kelvinox MX40, from Oxford Instruments), with base temperature 30mK, and an AVS47 resistance bridge. A program was developed to control the power supplied to the mixing chamber of the refrigerator, in order to perform temperature sweeps as slow as 1.7mK per hour; these allow characterization of very sharp transitions. The dilution refrigerator houses two sample holders: one, for 4-probe measurements, allows characterization of six samples at a time; a second one allows characterization of a TES in the same cooling run.

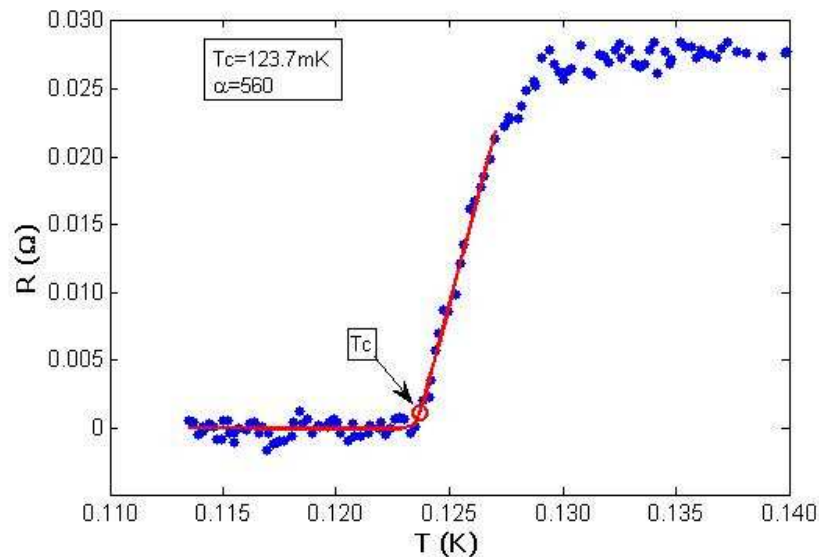


Figure 2. Transition of a Mo/Au TES with $T_c=123.7\text{mK}$ and $\alpha=560$. The solid line is the fit used to obtain these values, as described in the text. The critical temperature is indicated by a circle.

The TES is coupled to a sensor made of a 16-SQUID array provided by PTB (Physikalisch- Technische Bundersanstalt, Germany) and read with a Magnicon XXF-1 electronics box. The I-V curves are recorded both with positive and negative current allowing therefore the identification of eventual trapped magnetic fields in the setup. These fields can be compensated by a coil incorporated within the TES holder (providing 45mGauss/mA). The TES is nonetheless magnetically shielded with a lead can surrounded by μ -metal (Cryoperm). Finally, the electric signals are taken through RC filters at room temperature. At present work is in progress to perform complex impedance and noise measurements in the same setup with a spectrum analyzer, and to incorporate a ^{55}Fe radiation source with enough intensity to characterize the performance of full pixels as X-ray detectors, and in particular to measure their spectral resolution.

Fig.2 displays a typical transition of our TES. The critical temperature T_c , transition width ΔT and α values of the TES are obtained as follows: the transition is fitted to an exponential law followed by a linear dependence; T_c is defined as the temperature where both fits intercept. By forcing also the continuity of the first derivative, a three parameters fit is obtained from which a value for α is straightforwardly calculated. The fit is performed in a single step by introducing the Heaviside function $H(x)$:

$$R(T) = A [1 - H(T - T_c)] \exp[(T - T_c)/\Delta T] + A H(T - T_c) \left(1 + \frac{T - T_c}{\Delta T}\right)$$

where the fitting parameters are T_c , ΔT and A , and the parameter α , which characterizes the sharpness of the superconducting transition and is therefore directly related to the sensitivity of the TES sensor, is calculated as

$$\alpha \equiv \frac{d \log R}{d \log T} = \frac{T_c}{\Delta T}.$$

Usually, our TES display α values between 400 and 600, corresponding to transition widths between 2 and 6mK, although transitions as narrow as 1mK have also been recorded.

Fig.3 displays the calibrated I-V curves of a TES recorded at different bath temperatures. The TES transition corresponds the I-V points between the two straight lines, the vertical one and the finite slope one, representing respectively the superconducting and the normal states of the device. The TES will act as a microcalorimeter when biased in the transition zone. By fitting the power flow to the bath at different bath temperatures, the thermal conductivity G to the heat sink is obtained; good agreement with estimated G values for the used membrane thicknesses are obtained.

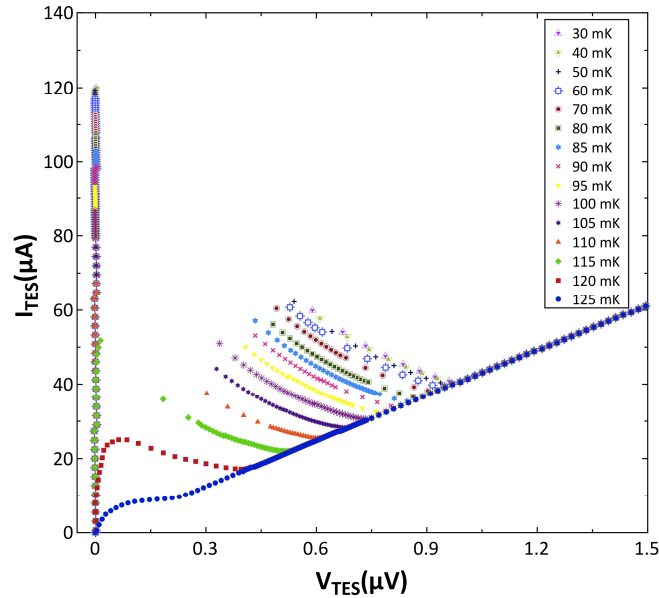


Figure 3. I-V curves at different bath temperatures of a TES with $T_c \sim 130\text{mK}$. I_{TES} and V_{TES} are respectively the current through and the voltage across the device.

3.2 Electrodeposited Bi films

We are in the process of optimizing Bi films, fabricated by chemical electrodeposition, intended to constitute the X-ray absorber. Electrode isolation, plating solution, method to control the deposition (either constant voltage V or constant current I, or pulsed techniques) and the V (I) used affect the morphology of the films, therefore modifying their mechanical and functional properties. As an example, Fig.4 displays Scanning Electron Microscopy (SEM) photographs of two films of similar thickness (~4 μm , close to what would be required to have a high quantum efficiency detector), deposited at different conditions. Films are polycrystalline, with grain sizes that can vary from around 1 μm to 10 μm ; the grain size distribution can also change significantly with the deposition conditions.

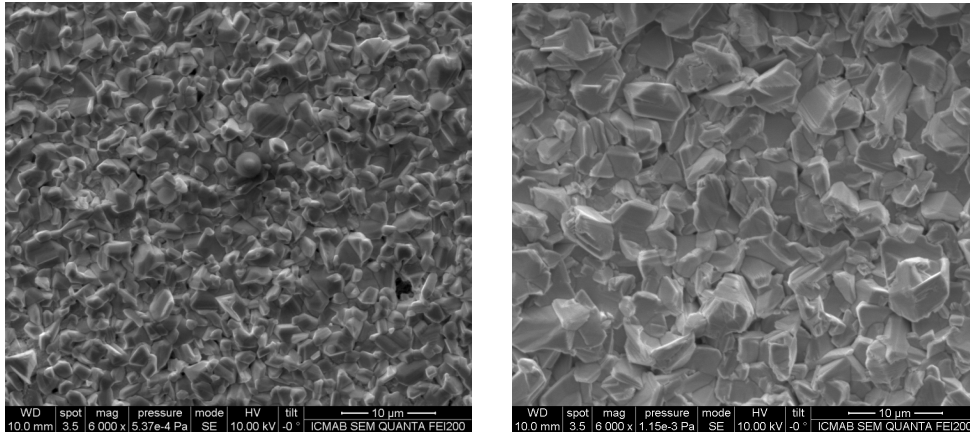


Figure 4. Scanning Electron Microscopy images of two electrodeposited Bi layers, 4 μm thick. Grain sizes between 1 μm and 10 μm are obtained depending on deposition conditions.

Materials to be used as X-ray absorbers for TES detectors are required not to affect the TES (changes in the transition) and have high thermal conductance. The absorber electrical resistivity must be carefully tuned in order not to perturb the performance of the TES, but at the same time providing high thermal (and therefore electrical) conductivity. Reliable direct measurements of thermal conductance in a thin film are quite difficult; this is particularly true for Bi films deposited on Au. This is why we are using resistivity measurements in the optimization process.

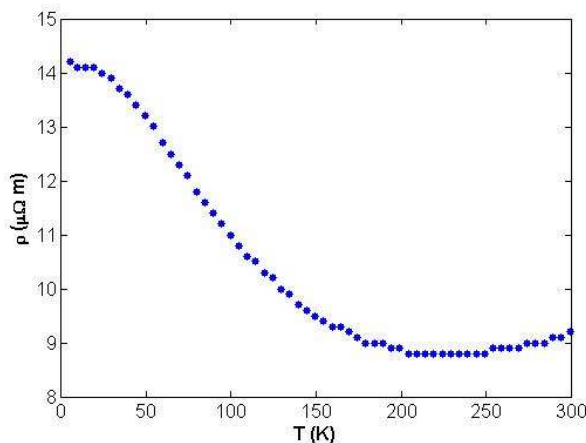


Figure 5. Resistance versus temperature of a 4 μm thick Bi layer deposited on Au(10nm)/Cr(2nm)/glass.

The temperature dependent resistance of films is measured using the four-probe method, in a commercial PPMS (Physical Property Measurement System) from Quantum Design; measurement of a Au(10nm)/Cr(2nm) bilayer,

identical to that underneath Bi films, shows that its contribution to the measured resistance when Bi is present is below 10%. Fig.5 displays a representative $R(T)$ curve of a 4 μm -thick Bi film. Room temperature resistivity values close to 10 $\mu\Omega\text{ m}$, one of magnitude larger than the nominal resistivity of Bi, are obtained. Although bulk Bi is a semimetal with very weak dR/dT , usually^{15,16,17} Bi films display semiconducting behavior as that shown in this figure. If we define $RRR=R(300\text{K})/R(4.2\text{K})$, the goal would be to obtain an RRR value as close to 1 as possible^{18,19}. Values of RRR around 0.7 are measured, but strategies to further reduce this and the room temperature resistance are also being addressed.

4. CONCLUSIONS AND FUTURE WORK

We are developing X-ray detectors constituted by Mo-based TES, with the aim of providing highly performant TES front-end sensor arrays for the X-IFU instrument on Athena. We have already obtained and made the first dark characterization of TES microcalorimeters with T_c around the operating temperature 100mK; work in progress is focused on the optimization of electrodeposited Bi films to be used as absorbers, building the setup for complex impedance and noise measurements, and improving TES layouts as well as streamlining fabrication procedures.

Several single pixel layouts have been designed and will soon be tested. The first goal is to analyse the effects on the TES transition and performances of the TES and pad contact geometry, and the effects of using either Mo or Nb for the superconducting pads and wiring. A further goal will be comparison of Mo/Au and Ti/Au TES with identical designs. We aim also at analysing the effect of the basic superconducting parameters of the proximity bilayers on the TES transition, in order to assist in the choice of best operating conditions in terms of temperature and magnetic field.

ACKNOWLEDGEMENTS

This work has been financed by the Spanish Ministerio de Economía y Competitividad, through project AYA2012-39767-C2-01. We thank PTB for providing the SQUIDs and for helpful discussions.

REFERENCES

- [1] Nandra, K., Barret, D., Barcons, X., Fabian, A., den Herder, J.-W., Piro, L., Watson, M., Adami, C., Aird, J., Afonso, J. M., and et al., "The Hot and Energetic Universe: A White Paper presenting the science theme motivating the Athena+ mission," 2013arXiv1306.2307N (June 2013).
- [2] Ravera, L. et al., "The X-ray Integral Field Unit (X-IFU) for Athena", in these proceedings.
- [3] Kaastra, J., Finoguenov, A., Nicastro, F., Branchini, E., Schaye, J., Cappelluti, N., Nevalainen, J., Barcons, X., Bregman, J., Croston, J., Dolag, K., Ettori, S., Galeazzi, M., Ohashi, T., Piro, L., Pointecouteau, E., Pratt, G., Reiprich, T., Roncarelli, M., Sanders, J., Takei, Y., and Ursino, E., "The Hot and Energetic Universe: The missing baryons and the warm-hot intergalactic medium", arXiv1306.2324K (June 2013).
- [4] Ettori, S., Pratt, G. W., de Plaa, J., Eckert, D., Nevalainen, J., Battistelli, E. S., Borgani, S., Croston, J. H., Finoguenov, A., Kaastra, J., Gaspari, M., Gastaldello, F., Gitti, M., Molendi, S., Pointecouteau, E., Ponman, T. J., Reiprich, T. H., Roncarelli, M., Rossetti, M., Sanders, J. S., Sun, M., Trinchieri, G., Vazza, F., Arnaud, M., Boeringer, H., Brighenti, F., Dahle, H., De Grandi, S., Mohr, J. J., Moretti, A. and Schindler, S., "The Hot and Energetic Universe: The astrophysics of galaxy groups and clusters", arXiv1306.2322E (June 2013).
- [5] Croston, J. H., Sanders, J. S., Heinz, S., Hardcastle, M. J., Zhuravleva, I., Birzan, L., Bower, R. G., Brüggén, M., Churazov, E., Edge, A. C., Ettori, S., Fabian, A. C., Finoguenov, A., Kaastra, J., Gaspari, M., Gitti, M., Nulsen, P. E. J., McNamara, B. R., Pointecouteau, E., Ponman, T. J., Pratt, G. W., Rafferty, D. A., Reiprich, T. H., Sijacki, D., Worrall, D. M., Kraft, R. P., McCarthy, I., and Wise, M., "The Hot and Energetic Universe: AGN feedback in galaxy clusters and groups", arXiv1306.2323C (June 2013).
- [6] Sciortino, S., Rauw, G., Audard, M., Argiro, C., Chu, Y.-H., De Becker, M., Drake, J., Feigelson, E., Gosset, E., Grosso, N., Guédel, M., Guerrero, M., Hervé, A., Kastner, J., Montez, R., Nazé, Y., Oskinova, L., Stelzer, B., and ud-Doula, A., "The Hot and Energetic Universe: Star formation and evolution", arXiv1306.2333S (June 2013).
- [7] Gottardi, L. et al., "Development of TES-based detectors array for the X-ray integral field unit (X-IFU) on the future X-ray observatory ATHENA", in these proceedings.

- [8] Bandler, S.R., Adams, J.S., Bailey, C.N., Busch, S.E., Chervenak, J.A., Eckart, M.E., Ewin, A.E., Finkbeiner, F.M., Kelley, R.L., Kelly, D.P., Kilbourne, C.A., Porst, J-P., Porter, F.S., Sadleir, J.E., Smith, S.J. and Wassell, E.J., "Advances in small pixel TES-based X-ray microcalorimeter arrays for solar physics and astrophysics", *IEEE Trans. on Appl. Supercond.* 23, 2100705 (2013).
- [9] Dirks, B.P.F., Popescu, M., Bruijn, M., Gottardi, L., Hoevers, H.F.C., de Korte, P.A.J., van der Kuur, J., Ridder, M. and Takei, Y., "TiAu-based micro-calorimeters for space applications", *Nucl. Instrum. Meth. A* 610, 83-86 (2009).
- [10] Fàbrega, L., Fernández-Martínez, I., Gil, O., Parra-Borderías, M., Camón, A., Costa-Krämer, J.L. González-Arrabal, R., Sesé, J., Briones, F., Santiso, J., and Peiró, F., "Mo-based proximity bilayers for TES: microstructure and properties", *IEEE Trans. on Appl. Supercond.* 19(6), 460-464 (2009).
- [11] Fabrega, L., Fernández-Martínez, I., Parra-Borderías, M., Gil, O., Camón, A., González-Arrabal, R., Santiso, J., Sesé, J., Costa-Krämer, J.L. and Briones, F., "Effects of stress and morphology on the resistivity and critical temperature of room-temperature sputtered Mo thin films", *IEEE Trans. on Appl. Supercond.* 19(6), 3779-3785 (2009).
- [12] Parra-Borderías M., Fernández-Martínez, I., Fàbrega, L., Camón, A., Gil, O., Costa-Krämer, J.L., González-Arrabal, R., Sesé, J., Bueno, J. and Briones, F., "Characterization of a Mo/Au thermometer for ATHENA", *IEEE Trans. on Appl. Supercond.* 23, 2300405 (2013).
- [13] Parra-Borderías M., Fernández-Martínez, I., Fàbrega, L., Camón, A., Gil, O., González-Arrabal, R., Sesé, J., Costa-Krämer, J.L., Warot-Fonrose, B., Serin, V. and Briones, F., "Thermal stability of Mo/Au bilayers for TES applications", *Supercond. Sci. and Technol.* 25, 095001 (2012).
- [14] Tralshawala, N. et al., "Fabrication of Mo/Au Transition-Edge sensors for X-ray spectrometry", *IEEE Trans. on Appl. Supercond.* 11(1), 755-758 (2001).
- [15] Hoffman, C., Meyer, J., Bartoli, F., Di Venere, A., Yi, X., Hou, C., Wang, H., Ketterson, J. and Wong, G., "Semimetal-to-semiconductor transition in bismuth thin films". *Phys. Rev. B* 48 (15), 11431-11434 (1993).
- [16] Yang, F.Y., Liu, K., Hong, K., Reich, D.H., Searson, P.C. and Chien, C.L., "Large magnetoresistance of electrodeposited single-crystal bismuth thin films", *Science* 284, 1335-1337 (1999).
- [17] Inoue, M., Tamaki, Y. and Yagi, H., "Transport properties of bismuth films", *J. Appl. Phys.* 45, 1562-1566 (1974).
- [18] Brown, A.D., Bandler, S.R., Brekosky, R., Chervenak, J.A., Figueroa-Feliciano, E., Finkbeiner, F., Iyomoto, N., Kelley, R.L., Kilbourne, C.A., Porter, F.S., Smith, S., Saab, T., and Sadleir, J., "Absorber materials for Transition-Edge Sensor X-Ray microcalorimeters", *J. Low Temp. Phys.* 151, 413-417 (2008).
- [19] Bruijn, M.P., Ridder, M.L., Krouwer, E., Hoevers, H.F.C., de Korte, P.A.J. and van der Kuur, J., "Progress in fabrication of microcalorimeter arrays: X-ray absorbers and high-density stripline wiring", *Nucl. Instrum. Meth. A* 559, 444-446 (2006).